Paper Number:
Session Topic:

Title: **Quantification of Error Associated with Using Misaligned Meshes in Continuum Damage Mechanics Material Models for Matrix Crack Growth Predictions in Composites**

Authors: Brian Justusson
Imran Hyder
Stewart Boyd
Frank Leone

ABSTRACT

The ability of a material model to capture in-plane matrix mode I and mode II crack growth is an essential component for modeling ply level damage evolution in composite structures. Previous studies using a continuum damage mechanics (CDM) approach have shown success in satisfying benchmark solutions for mode I and II crack growth. However, success was shown using a fiber-aligned meshing strategy, which encourages matrix cracks to propagate in a single band of elements, along the fiber direction. Generating a fiber-aligned mesh becomes a highly involved process for laminates including off-axis (non 0° or 90°) plies. The objective of this study is to quantify the effect of non-fiber aligned mesh discretization on predictions of in-plane matrix crack propagation. The approach taken incrementally varies the mesh orientation angle relative to the fiber orientation; more specifically, misaligned meshes are used to quantify the effect of element angle orientation relative to the initial crack orientation on the energy released during matrix crack propagation simulations using a CDM method. CDM solutions obtained with the misaligned meshes are evaluated against known benchmarks for mode I and II matrix crack growth. The CDM solutions reveal a near-polynomial trend of increased predicted failure stress with increased mesh misalignment angle; hence implying a potential relationship between element orientation angle and apparent fracture toughness.

INTRODUCTION

Emerging Progressive Damage and Failure Analysis (PDFA) methods have potential to reduce the timeline for certification of new aerospace composite structures. Recently, United States government sponsored programs have been focused on the development and evaluation of these methods for applications of interest. The

Composite Airframe Life Extension (CALE) program from the Wright Patterson Air Force Research Laboratory has examined the use of these tools on bolted structures [1], [2]. Further, the NASA Advanced Composites Project (ACP) has chartered the goal of improving methods for targeted applications of fatigue, post-buckled stiffened panels with barely visible impact damage [3], and high energy dynamic impact [4].

In Phase I of the ACP, selected state-of-the-art PDFA methods were identified and preliminary analyses were performed to evaluate their predictive capability [3]. By considering the material model and previous work by Schaefer and Razi for intralaminar behavior [5], and by Krueger for interlaminar behavior [6], an efficient framework was developed to verify the functionality of the PDFA codes. When considering only the intralaminar response, state-of-the-art material models generally follow the A-B-C-D stress/strain response (Figure 1), including:

1. Elastic response (Region A);
2. Pre-peak non-linear response (Region B);
3. Element failure criteria (Region C); and
4. Element failure behavior or post-peak response (Region D).

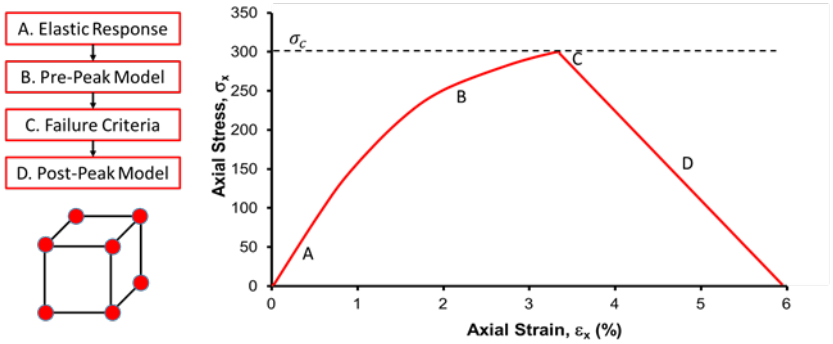

Figure 1. Stress/strain response regions of a common PDFA material model [5].

For continuum damage mechanics (CDM) approaches, a fracture energy based post-peak response is widely accepted for element failure behavior. This fracture energy based post-peak response is used in the research codes Enhanced Schapery Theory [7], CDMat [8], CompDam [9], rX-FEM [10], A-FEM [11], Floating Node Method [12], and NCYL [13], as well as in commercial software tools (e.g., Helius PFA [14], LS-DYNA MAT261 [15], Abaqus Hashin [16],). The post-peak response in these codes is formulated such that a cohesive law governs region D of the constitutive response. The law is defined by a two-parameter traction separation law that requires a strength and fracture toughness value for each mode of deformation. The reason for this fracture energy based post-peak response is two-fold:

1. By normalizing the area under the curve by the characteristic length of the element, a mesh size objective material model can be achieved. It has been shown that selection of a characteristic element length is critical to dissipating the correct amount of fracture energy [17].
2. Fracture mechanics appears to be an acceptable material model when long damage develops.

Critical to the long term success of PDFA methods is the ability to predict long damage. Long damage observed as matrix cracking/splitting (mode I/II respectively), such as that observed from a notch, can act as a strain relief mechanism [18]. The ability of a PDFA method to capture this strain relief is critical to establishing predictive capability for matrix damage and subsequent interaction with interlaminar damage. Linear Elastic Fracture Mechanics (LEFM) approaches, e.g., the Virtual Crack Closure Technique (VCCT), have been demonstrated for predicting long crack growth behavior, but require an initial flaw or a singularity to meet the requirement of an infinite stress state in front of the crack tip. CDM PDFA approaches on the other hand have been demonstrated to be able to predict the onset of damage and growth of damage up to the point where LEFM may be applicable. This is accomplished through the material model that allows the transition between strength based propagation and fracture based propagation.

To evaluate the ability of PDFA methods to propagate long damage, an LEFM solution for a center-cracked anisotropic plate loaded in tension, as seen in Figure 2a, was established as a benchmark by Mabson et al. in [19]. In this study the effect of varying release pressure (i.e., input material strength) on the predicted failure stress was evaluated. Leone et al. extended the work in by including Mode II boundary conditions, as shown in Figure 2b [20]. Leone et al. used fiber-aligned meshes and demonstrated, for the meshes considered, that a CDM approach can satisfy the benchmark solutions for mode I and mode II crack growth. In addition, two critical issues associated with evaluation of CDM PDFA methods for matrix crack propagation were noted in [21]:

1. Release pressures are generally not varied with CDM approaches due to a material strength being used as an effective release pressure. While selection of the release pressure may have little effect on long damage growth predictions, improper selection will affect the predicted onset of damage. To remedy this, Leone proposed the use of a constant release pressure in combination with a range of appropriate element sizes.

2. To evaluate the CDM approach, the initial crack must be modeled within the continuum damage mechanics framework (i.e., the initial crack is modeled by fully damaged elements).

Generating a fiber-aligned mesh becomes a highly involved process for laminates including off-axis (non 0° or 90°) plies and may not be practical for large structures. However, quantification of the error associated with using a misaligned mesh in a CDM simulation of matrix crack propagation has not been fully established. The objective of this study is therefore to quantify the error associated with using CDM based PDFA approaches with misaligned meshes for matrix crack propagation. The error is quantified by comparing analysis predictions for two-piece failure stress with the values obtained from the pure mode I and mode II matrix crack growth benchmark solutions provided in Refs. [19] and [20]. In a series of analyses, the element orientation angle relative to the fiber direction is incrementally increased, and the finite element analysis results are compared with the closed-form benchmark solutions.

This paper discusses the technical approach taken in the study, provides a quantitative comparison between the finite element solutions and the mode I and mode II benchmarks, discusses the implications of the relationship between misaligned meshes and long damage growth, and finally provides a conclusion on the findings.

TECHNICAL APPROACH

In this study, a representative CDM based PDFA method was evaluated against benchmarks established for Center Notch Tension (CNT) and Center Notch Shear (CNS) problems. The benchmarks are analytical LEFM mode I and mode II matrix crack growth solutions for CNT and CNS coupons, and were obtained from references [19] and [20]. The CNT and CNS specimen boundary conditions are shown in Figures 2a and 2b, respectively. The center notch specimens are unidirectional panels, with the fiber orientation parallel to the crack. The geometry of the center notch specimens is 127 mm by 127 mm with a 25.4 mm crack. The CDM method used in this study was CompDam [21]. CompDam was considered technically mature since it was successful in predicting long matrix crack damage growth in previous similar studies [20]. The ability to accurately predict long matrix crack damage growth is enabled in CompDam by the inclusion of the Deformation Gradient Decomposition (DGD) algorithm, which ensures accurate definition of the material coordinate frame and crack surfaces in Abaqus during large shear-dominant element deformation [21]. CompDam is implemented as an Abaqus/Explicit user material subroutine (VUMAT). The source code for CompDam is available at https://github.com/nasa/CompDam_DGD.

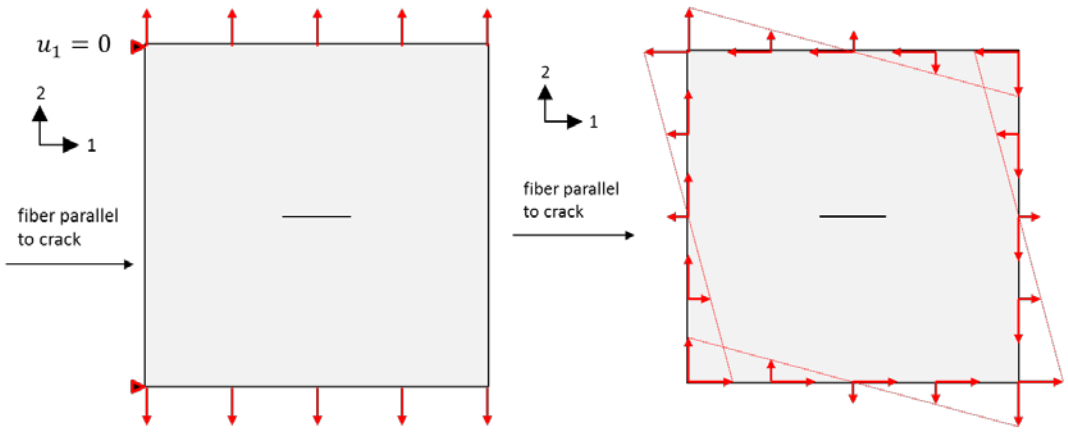

a. Center Notch Tension b. Center Notch Shear

Figure 2. Schematics for the Center Notch Tension and Center Notch Shear benchmark problems.

A finite element model (FEM) of the center notch problem described in references [19] and [20] used structured meshes that were aligned with the initial fiber and matrix material directions, i.e., fiber aligned. The effect of misaligned meshes on predictions of matrix crack propagation and two-piece failure stress was quantified by incrementally increasing the angle between the mesh orientation and the material fiber direction, creating a misaligned mesh. The angle θ between the mesh orientation and the material fiber direction, Figure 3, is referred to as the misalignment angle. The misalignment angle was swept from 0° to 90° in increments of 5°.

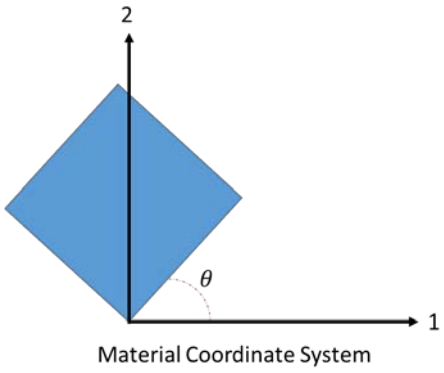

Figure 3. Definition of misalignment angle, θ.

For each misalignment angle, a mesh was generated for the CNT and CNS problems. Elements with fixed edge lengths of 0.20 mm were used, based on the recommendations from the study conducted in Ref. [20]. The initial crack was represented in the simulations by a band of fully damaged elements. The far-field stresses were obtained at predicted two-piece failure and at damage initiation. Two-

piece failure stress was defined as the stress level where a load drop was observed and where the crack band spanned the width of the model. Initiation stress was defined as the first instance of a non-zero damage variable occurring immediately ahead of the crack tips. The far-field stress was recorded from the top left element highlighted in red in Figure 4. Following on the approach of Leone et al. [20], the FEM simulation was considered to have successfully predicted the benchmark solution when the predicted two-piece failure stress was within 10% of the corresponding LEFM benchmark solution.

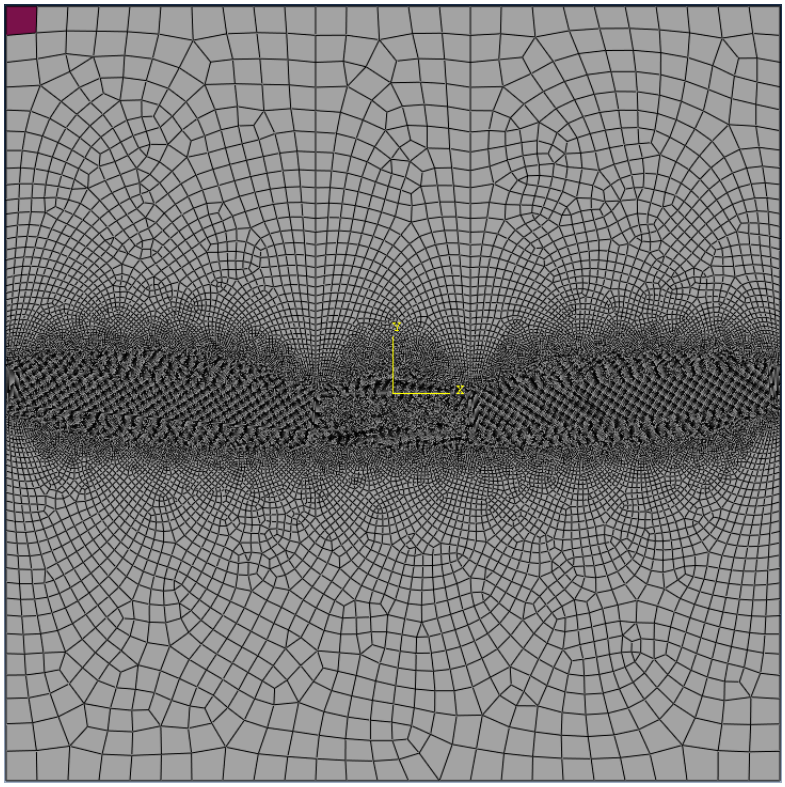

Figure 4. Top left element, shown in red, used to extract far-field stresses σ_{22} (mode I) and τ_{12} (mode II) corresponding to crack damage initiation and two-piece failure.

RESULTS: MODE I LOADING

The results of the mode I misaligned mesh study are shown in Figure 5. Predicted damage initiation stress and two-piece failure stress are shown as a function of misalignment angle, with the failure stress ±10% of the LEFM shown by the green banded region. The results indicate that the predicted initiation stress for mode I failure is insensitive to mesh orientation; however, the predicted two-piece failure stress generally increases with misalignment angle. The failure stress versus mesh misalignment angle shows a general parabolic trend. For mesh misalignment angles of ±15°or less, the success criterion is met. When the misalignment angle is larger

than 15°, the apparent fracture energy is over predicted, resulting in over prediction of the two-piece failure load. The highest predicted two piece failure stress occurs at a misalignment angle of 45° (maximum misalignment).

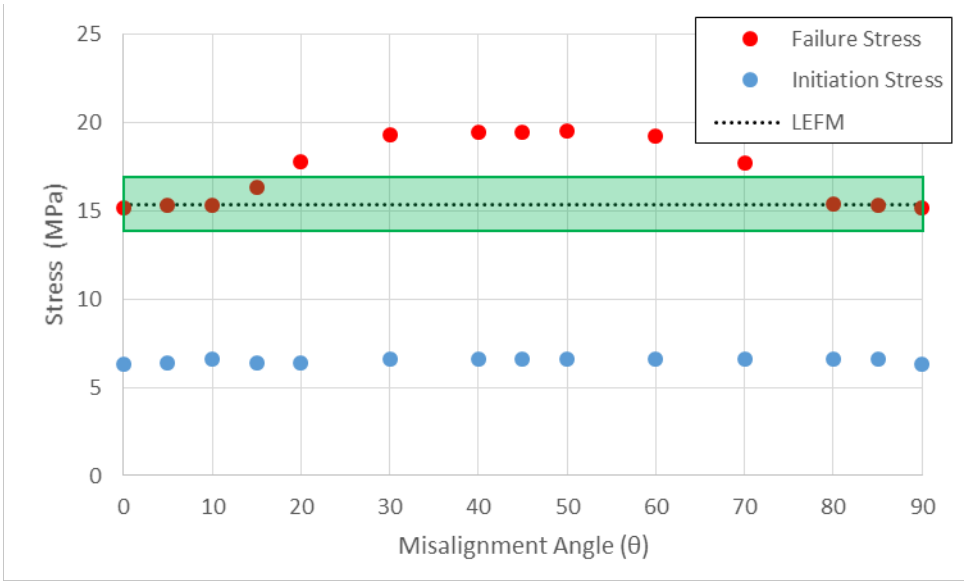

Figure 5. Results of mode I misaligned mesh study.

Evaluation of the predicted crack path is necessary to interpret the results provided in Figure 5. The crack path has two key features related to CDM: (1) the direction of crack propagation, and (2) the development of a fracture process zone (FPZ). The direction of crack propagation can be either self-similar or non-self-similar. A self-similar crack is a crack that develops equally on both sides of the initial crack and propagates along the initial orientation of the crack, which, for these models, is aligned with the material fiber direction. A non-self-similar crack will not follow the material coordinate system, and will instead be affected by the orientation of the mesh lines, if not following the mesh lines outright. The predicted path of the propagated cracks was self-similar for each of the misaligned meshes (Figure 6).

Figure 6 also shows the fully developed FPZ corresponding to each of the misaligned meshes used in the study. The FPZ was identified by examining the matrix damage variable. Upon initiation of damage, the CompDam matrix damage variable, *D2*, becomes non-zero. The damage front evolves and the FPZ is fully developed when the first element returns a *D2* value of 1.0. The length of the FPZ, L_{fpz}, was measured as the distance between an element that has completely released and the furthest element with a non-zero matrix damage state variable, Figure 7. In Figures 6 and 7, any element that is depicted as red has entered into the post-peak response of the material model (i.e. damage state variable greater than zero) whereas elements that are completely removed have been fully damaged (i.e., damage state variable equals

1). Elements were not removed using element deletion during the simulations, rather they are just visually removed for clarity.

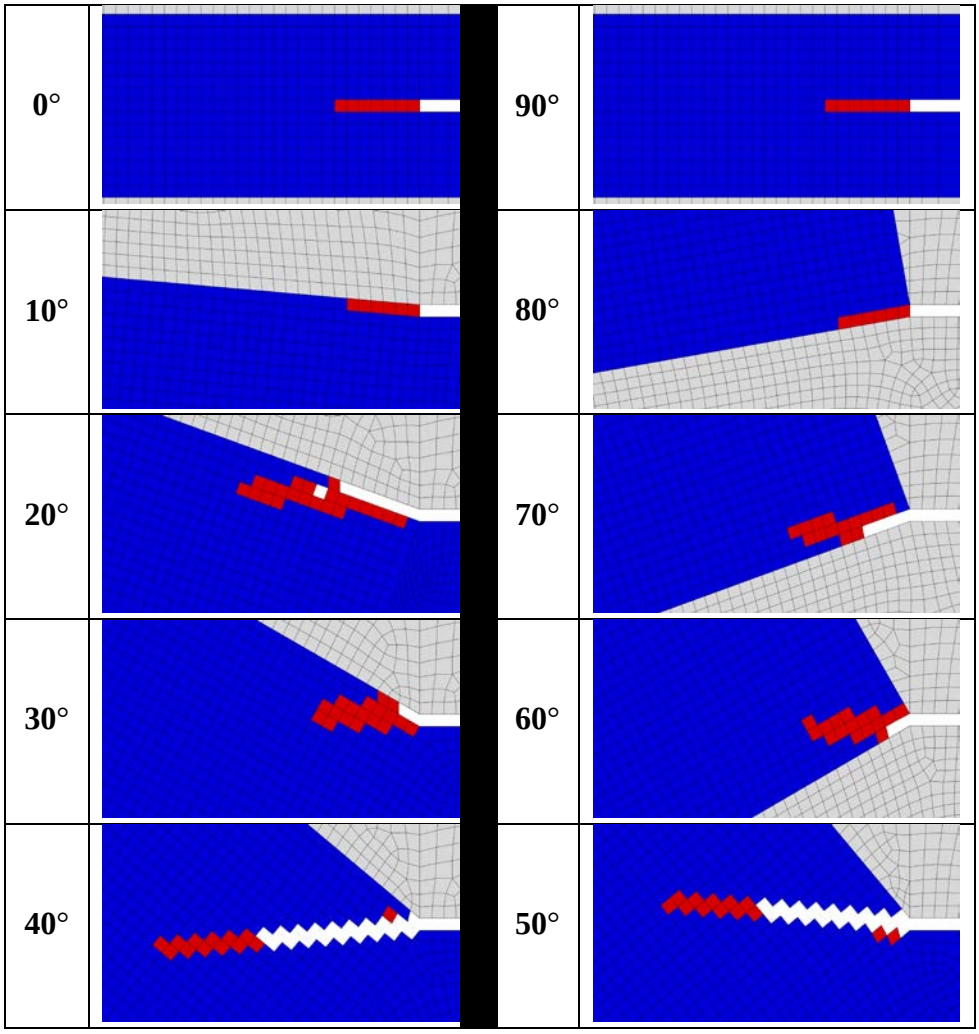

Figure 6. Fracture process zone corresponding to different mesh misalignment angles, mode I loading.

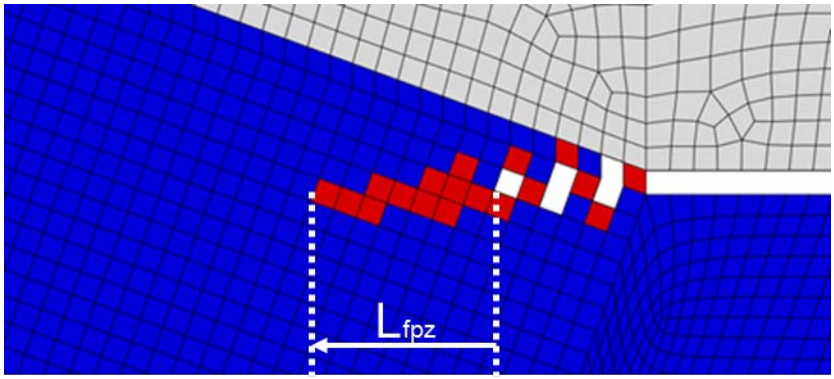

Figure 7. Measurement of the length of the fracture process zone (20° misalignment angle). Fully damaged elements are pictorially removed for clarity.

Figure 8 shows two sets of measurements of the FPZ: (1) the total number of elements in the FPZ, (2) the length of the FPZ. The length of the process zone is shown to vary between 1.18 mm and 2.20 mm with the longest process zones generally correlating with higher element misalignment angles. Additionally, the number of elements in the process zone increases with higher misalignment angle; however, the height of the process zone also increases with misalignment angle. For example, as shown in Figure 6, there is one element across the height of the process zone for the mesh with a 0° misalignment angle, but there are generally three elements along the process zone height for the mesh with a 40° misalignment angle. The increased height of the process zone for higher misalignment angles has two effects: (1) each row of elements along the height of the process zone dissipates energy as if it represents the crack path, increasing the total energy dissipated during crack propagation, and (2) the increased height of the process zone acts as a blunting mechanism, delaying damage initiation and potentially increasing predicted far-field failure stress relative to the benchmark solution.

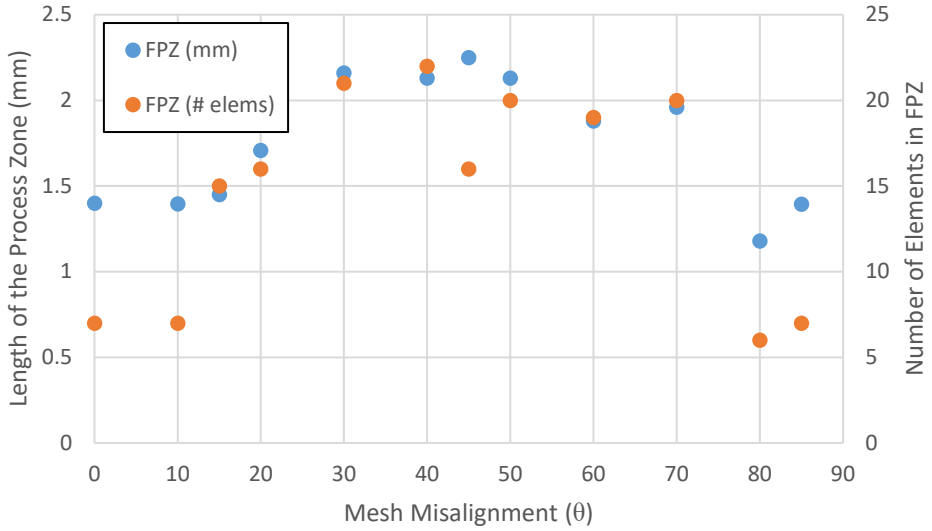

Figure 8: Length (distance and element count) of the fracture process zone as a function of mesh misalignment angle, mode I loading.

RESULTS: MODE II LOADING

The results of the misaligned mesh study for mode II loading are shown in Figure 9. The results are similar to those for the mode I loading, with the success criterion being met with mesh misalignments of ±10°. The results indicate that the initiation stress for mode II loading is relatively insensitive to mesh orientation; however, the two-piece failure stress, generally, increases with mesh misalignment. The response shows a characteristic parabolic response with a local peak in predicted failure stress for 30° and 60° misalignment angles. All of the simulations exhibited an unstable fracture event.

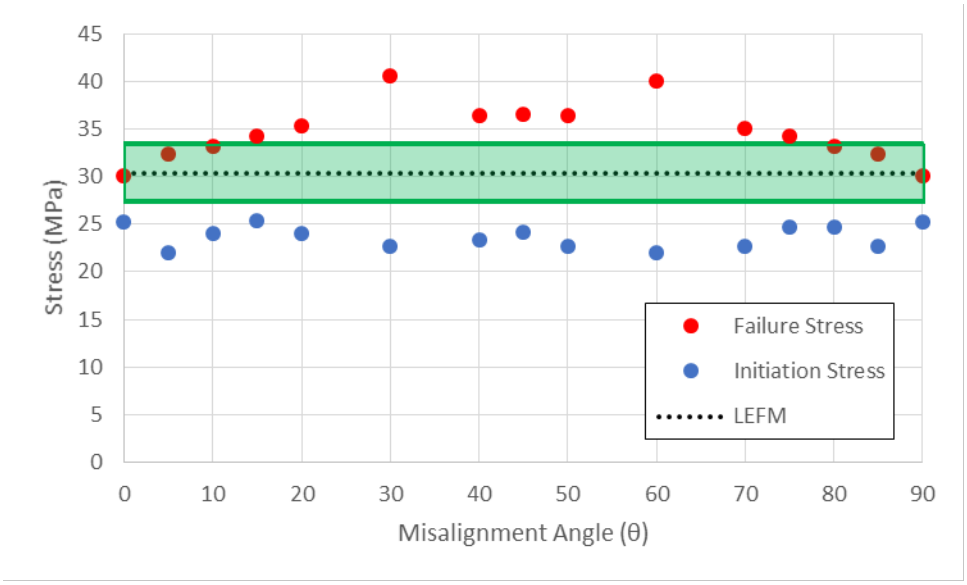

Figure 9. Results of mode II misaligned mesh study.

In order to better understand the effect of the misaligned mesh on the results summarized in Figure 9, the FPZ is again plotted in Figure 10. The crack behavior was self-similar and propagated along the material coordinate system direction. As with the mode I results, elements shown in red indicate that the post-peak response has been initiated, and non-displayed elements indicate that the post-peak fracture energy has been fully dissipated.

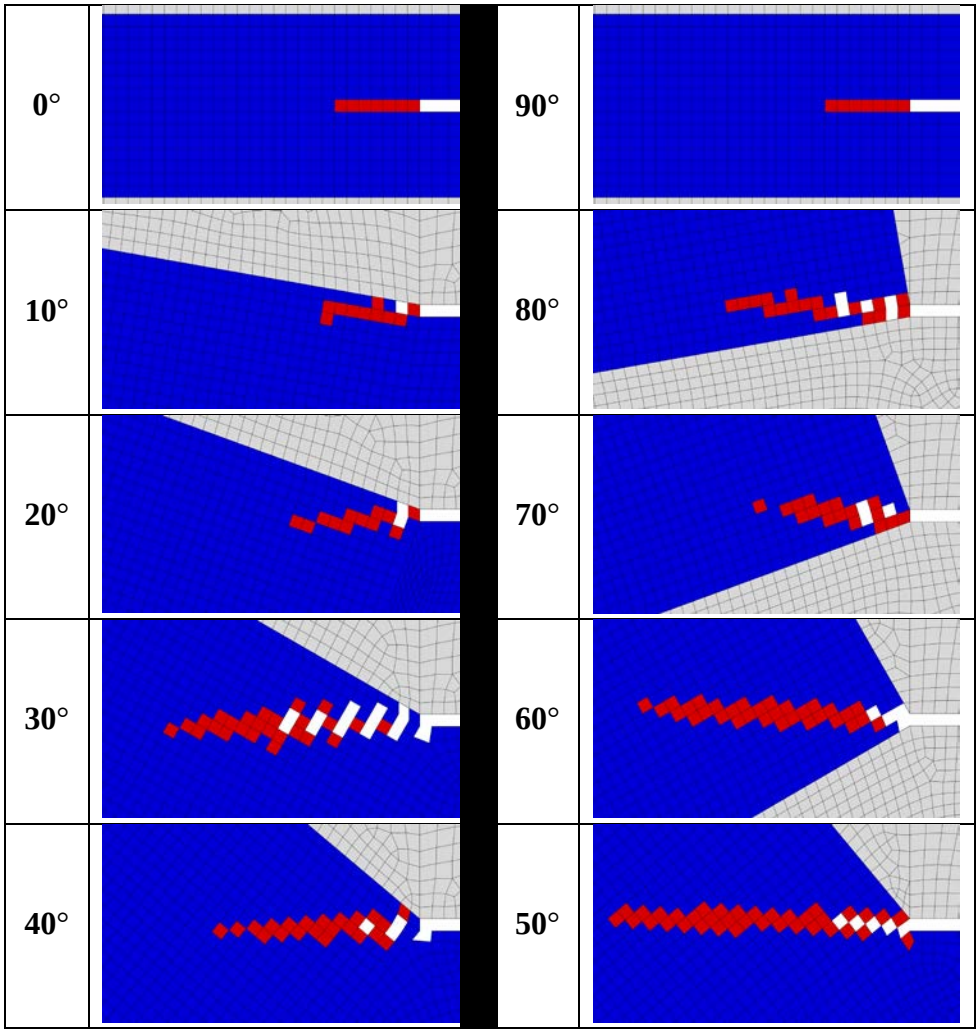

Figure 10. Fracture process zone corresponding to different mesh misalignment angles, mode II loading.

From Figure 10, the length of the FPZ can be measured with respect to the material coordinate system direction. Figure 11 shows a comparison between the length of the FPZ and the number of elements in the process zone with varying mesh misalignment angle. The length of the process zone varies between 1.2 mm to 4.4 mm. The number of elements in the height of the process zone is less for mode II than it is for mode I. The number of elements in the process zone and the size of the process zone are largest for mesh misalignment angles of 30° and 60°.

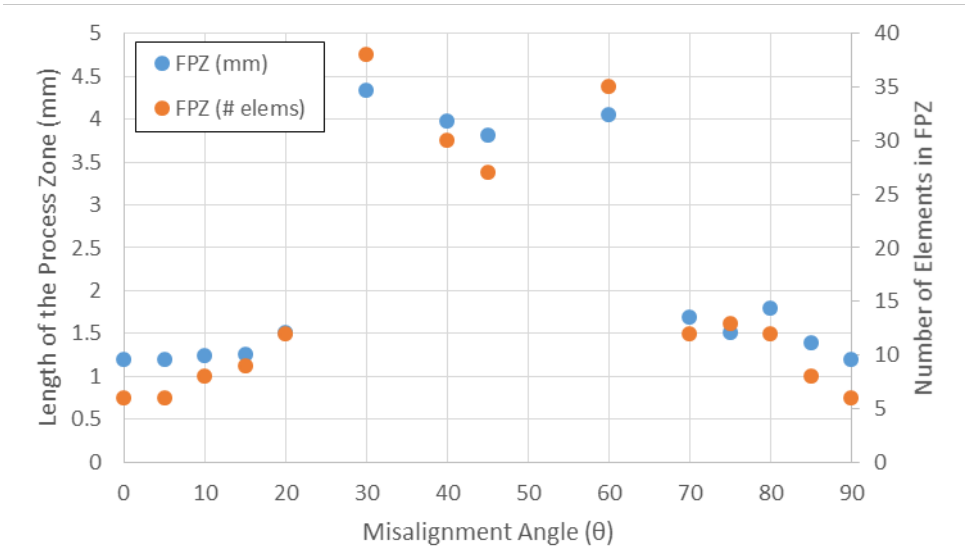

Figure 11. Length (distance and element count) of the fracture process zone as a function of mesh misalignment angle, mode II loading.

The large process zone length and the large number of elements in the process zone were shown to be a result of crack-tip blunting occurring at the notch tip, Figure 12. Results shown in Figure 12 for the 30° mesh misalignment case show self-similar crack growth behavior on one side of the coupon and crack blunting on the other side of the coupon. The blunted crack-tip leads to a high apparent fracture toughness that results in a high predicted two piece failure stress compared to the benchmark solution.

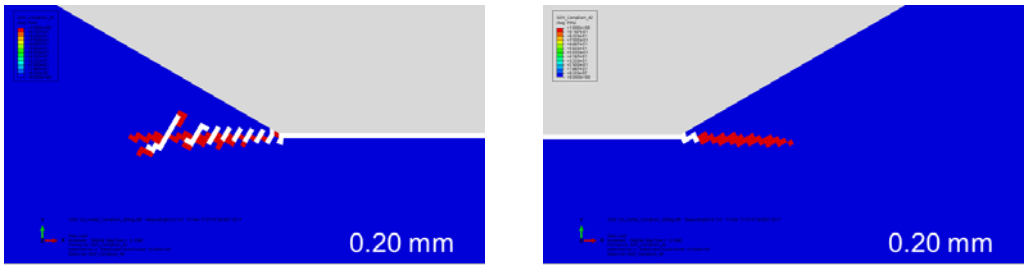

Figure 12. Representative fracture process zones at the two crack tips for mesh misalignment angles of 30° and 60°. Non-self-similar crack growth was observed on only one side of the coupon.

Additional investigation found the following for the 30° and 60° misaligned meshes:

1. The side of non-self-similar crack growth is dependent on the sign of the shear;
2. The same effect was observed for repeated analyses with reduced element size; and
3. The same effect was observed with the same misalignment of the mesh on the left and right side of the center crack.

DISCUSSION

PDFA methods, and in particular CDM methods, have a wide variety of best practices that result in restrictive mesh limitations including aligned meshing strategies. In some cases such as open hole tension/compression coupons, it is desirable to have a radial mesh around the hole to capture stress concentrations and allow for coarsening of the mesh away from the stress-riser [22]. Similarly, it is desirable to have a single intralaminar mesh to represent all plies in order to reduce the use of 6-noded linear triangular elements and tie definitions. Should an end user elect to not follow best practices in favor of ease of modeling, it may result in inaccurate simulations of the material response.

While CompDam is characteristic of a continuum, lamina-level fracture based PDFA approach, other method developers have noted that the problem may be related to the calculation of the characteristic element length [17]. There is a need for these methods to capture both the effective energy and self-similar behavior of a crack to improve predictive capability and to relax restrictive meshing requirements.

Abaqus based methods, such as CompDam, can utilize an internal subroutine called VUCHARLENGTH to define the characteristic element length. By default, VUCHARLENGTH returns a value based on the geometric mean, i.e., a typical length of a line across the element, though more elaborate definitions can be written by the user. Similarly, LS-DYNA approaches like MAT261 use a characteristic element length that is based on the ratio of volume to the maximum projection area. In both of these cases, the fracture energy may not be accounted for appropriately for misaligned meshes.

The problem is further exacerbated through the inclusion of additional elements within the FPZ. There is a geometric minimum element size that is required to propagate a crack. When the crack has a “spill-over” effect, it allows for additional energy to be introduced into the failure process. This is best shown in Mode I results where the misalignment was increased and there was significant spill-over into adjacent rows of elements, creating a blunted crack tip. These results were not observed in the Mode II case.

The effects of both additional elements in the FPZ and the internal calculation of characteristic element length is not always clear in terms of contribution. Considering the 45° misaligned mesh for Mode II in which the apparent fracture energy is high, the crack path already has the minimum number of elements to propagate through the mesh in a self-similar fashion. Further, the FPZ is relatively large compared to the 0° mesh, indicating that more elements are required to enter into release prior to fracture propagation. This result is consistent with previous findings that the FPZ size

increases with increasing toughness and indicates that the fracture energy might not be accounted for correctly by normalizing by the length returned by the default characteristic element length measures. Additional corrections to the definition of the characteristic element length may be required to ensure that the results are energetically consistent regardless of mesh orientation and element size.

CLOSING REMARKS

The ability of a characteristic continuum, lamina-level fracture based PDFA method to predict long in-plane matrix damage growth was evaluated for mode I and mode II loading. Analyses of unidirectional center notched tension (CNT) and center notched shear (CNS) coupons were conducted with FEMs where the mesh orientation was varied with respect to the material coordinate directions. Analysis predictions were compared to previously developed closed-form LEFM benchmark solutions for the CNT and CNS coupons. Under both mode I and mode II loading conditions, the simulation results for two-piece failure stress were within 10% of the benchmark solution for misalignment angles of 10° or less. For larger misalignment angles, the simulations over predicted the benchmark solutions. As the mesh misalignment angle increased, the number of elements in the FPZ and the length of the FPZ were shown to increase. These two factors suggest that the fracture energy dissipated during crack propagation is not being properly accounted for through the typical regularization with the characteristic element length.

Although the results of the study imply that using non fiber-aligned meshes with CDM-based PDFA methods to predict long matrix crack growth can yield inaccurate results, the quantification of error in two piece failure predictions performed in this study revealed a potential relationship between the material orientation and element misalignment angle. Since a higher element misalignment angle yielded a higher apparent fracture toughness, a modified, characteristic element size can be introduced into the material model's traction-separation law to compensate for the higher apparent fracture toughness. If an appropriate element misalignment to material orientation relationship can be captured within the computational model, the matrix crack growth predictions using CDM-based PDFA methods with unstructured meshes may be improved. Future work will involve determining a relationship between element misalignment angle and material orientation to address CDM issues with misaligned meshing strategies.

ACKNOWLEDGEMENTS

The material is based upon work supported by NASA under Award No. NNL09AA00A and 80LARC17C0004. Any opinions, findings, and conclusions or

recommendations expressed in this material are those of the author(s) and do not necessarily reflect the views of the National Aeronautics and Space Administration.

References

[1] C. Rousseau, S. Engelstad and S. Clay, "Data Requirements for Progressive Damage Analysis of Double-Shear Bearing in Composites," in *AIAA/ASCE/AHS/ASC Structures, Structural Dynamics, and Materials Conference*, Kissimmee, FL, 2018.

[2] J. Bartley-Cho, T. Palm and V. Ranatunga, "Overview of Composite Airframe Life Extension Program Project 2: Tools for Assessing the Durability and Damage Tolerance of Fastened Composite Joints," in *AIAA/ASCE/AHS/ASC Structures, Structural Dynamics, and Materials Conference*, Kissimmee, FL, 2018.

[3] S. Wanthal, J. Schaefer, B. Justusson, I. Hyder, S. Engelstad and C. Rose, "Verification and validation process for progressive damage and failure analysis methods in the NASA Advanced Composites Consortium," in *American Society for Composites Technical Conference*, West Layfayette, IN, 2017.

[4] K. Hunziker, J. Pang, M. Melis, J. M. Pereira and M. Rassaian, "NASA ACC High Energy Dynamic Impact Methodology and Outcomes," in *AIAA/ASCE/AHS/ASC Structures, Structural Dynamics, and Materials Conference*, Kissimmee, FL, 2018.

[5] H. Razi, J. Schaefer, S. Wanthal, J. Handler, G. Renieri and B. Justusson, "Rapid Integration of New Analysis Methods in Production," in *American Society for Composites Technical Conference*, Williamsburg, VA, 2016.

[6] R. Krueger, "A Summary of Benchmark Examples to Assess the Performance of Quasi-static Delamination Propagation Prediction Capabilities in Finite Element Codes," *Composite Materials*, vol. 49, no. 26, 2015.

[7] E. J. Pineda and A. M. Waas, "Enhanced Schapery Theory Software Development for Modeling Failure of Fiber-Reinforced Laminates," NASA Tech Brief , July 2013.

[8] Y. Nikishkov, A. Makeev and G. Seon, "Progressive Fatigue Damage Simulation Method for Composites," *International Journal of Fatigue*, vol. 48, pp. 266-279, 2013.

[9] C. A. Rose, C. G. Davila and F. A. Leone, "Analytical Methods for Progressive Damage of Composite Structures," NASA/TM-2013-218024, July 2013.

[10] E. Iarve, M. Gurvich, D. Mollenhauer, C. Rose and C. Davila, "Mesh-independent Matrix Cracking and Delamination Modeling in Laminated Composites," *International Journal For Numerical Methods in Engineering,* vol. 88, no. 8, pp. 749-773, 2011.

[11] D. Ling, Q. Yang and B. Cox, "An Augmented Finite Element Method for Modeling Arbitrary Discontinuities in Composite Materials," *International Journal of Fracture,* vol. 156, no. 1, pp. 53-73, 2009.

[12] N. De Carvalho, B. Chen, S. Pinho, P. Baiz, J. Ratcliffe and T. Tay, "Floating Node Method and Virtual Crack Closure Technique for Modeling Matrix Cracking-Delamination Interaction," NASA/CR-2013-218022, July 2013.

[13] D. Zhang and A. Waas, "Progressive damage and failure response of hybrid 3D textile composites subjected to flexural loading, part II: Mechanics based multiscale computational modeling of progressive damage and failure," *International Journal of Solids and Structures,* Vols. 75-76, pp. 321-335, 2015.

[14] D. Kenik, E. Nelson, D. Robbins and G. Mabson, "Developing Guidelines for Application of Coupled Fracture/Continuum Mechanics - Based Composite Damage Models for Reducing Mesh Sensitivity," in *AIAA/ASCE/AHS/ASC Structures, Structural Dynamics, and Materials Conference,* Honolulu, HI, 2012.

[15] Livermore Software Technology Corporation (LSTC), LS-DYNA Keyword User's Manual, vol. II, Livermore, CA, 2018.

[16] Dassault Systemes, *ABAQUS,* 2018.

[17] A. Joseph, P. Davidson and A. Waas, "Failure Analysis of Composite Multi-bolt Joints using Intra-Inter Crack Band Model (I2CBM)," in *AIAA/ASCE/AHS/ASC Structures, Structural Dynamics, and Materials Conference,* Kissimmee, FL, 2018.

[18] J. Schaefer, B. Justusson, M. Pike, A. Makeev and Y. Nikishkov, "Application of In-Situ Computed Tomography for Validation of Open Hole Fatigue Model Predictions," in *American Society for Composites Technical Conference,* West Lafayette, IN, 2017.

[19] G. Mabson, O. Weckner and M. Ramnath, "Finite Element Based Decohsive Failure Simulation Sensitvity Studies," in *AIAA/ASCE/AHS/ASC Structures, Structural Dynamics, and Materials Conference,* Honolulu, HI, 2012.

[20] F. A. Leone, C. G. Davila, G. E. Mabson, M. Ramnath and I. Hyder, "Fracture-Based Mesh Size Requirements for Matrix Cracks in Continuum Damage Mechanics Models," in *AIAA/ASCE/AHS/ASC Structures, Structural Dynamics, and Materials Conference,* Grapevine, TX, 2017.

[21] F. A. Leone, "Deformation Gradient Tensor Decomposition for Representing Matrix Cracks in Fiber-Reinforced Composite Structures," *Composites Part A: Applied Science and Manufacturing,* vol. 76, pp. 334-341, 2015.

[22] M. Pike, J. Schaefer, B. Justusson and S. Liguore, "Composite Laminate Progressive Damage Failure Analysis Benchmarking using High Fidelity Inspection Damage Maps," in *AIAA/ASCE/AHS/ASC Structures, Structural Dynamics, and Materials Conference,* Kissimmee, FL, 2018.